A resonance Raman study of new pyrrole-anchoring dyes for NiO-sensitized solar cells.

Gareth H. Summers[a,b], Grace Lowe[a], Jean-François Lefebvre[a], Simbarashe Ngwerume[a], Maximilian Bräutigam[c,d], Benjamin Dietzek[c,d]*, Jason E. Camp[a,e]*, Elizabeth A. Gibson[a,b]*

[a] School of Chemistry, The University of Nottingham, University Park, Nottingham, NG7 2RD, UK.

[b] School of Chemistry, Newcastle University, Newcastle upon Tyne, NE1 7RU, UK

[c] Leibniz Institute of Photonic Technology (IPHT) Jena e. V., Albert-Einstein-Str. 9, 07745 Jena, DE

[d] Institute for Physical Chemistry and Abbe Center of Photonics, Friedrich-Schiller University Jena, Helmholtzweg 4, 07743 Jena, DE

[e] Department of Chemical Sciences, University of Huddersfield, Queensgate, Huddersfield, HD1 3DH, UK.

Elizabeth.gibson@ncl.ac.uk

j.e.camp@hud.ac.uk

benjamin.dietzek@leibniz-ipht.de

Abstract

Three dyes for p-type dye-sensitised solar cells containing a novel doubly anchored pyrrole donor group were synthesised and their solar cell performances were evaluated. Dye **1** was comprised of a phenyl-thiophene linker and a maleonitrile acceptor, which has been established as an effective motif in other push-pull dyes. Two boron dipyrromethane analogues, dyes **2** and **3**, were made with different linker groups to compare their effect on the behaviour of these dyes adsorbed onto nickel oxide (dye|NiO) under illumination. The photo-excited states of dye|NiO were probed using resonance Raman spectroscopy and compared to dyes anchored using the conventional 4-aminobenzoic acid moiety (**P1** and **4**). All three components, the anchor, the linker and the acceptor group were found to alter both the electronic structure

following excitation and the overall solar cell performance. The bodipy acceptor gave a better performance than the maleonitrile acceptor when the pyrrole anchor was used, which is the opposite of the triphenylamine push-pull dyes. The linker group was found to have a large influence on the short-circuit current and efficiency of the p-type cells constructed.

TOC Image:

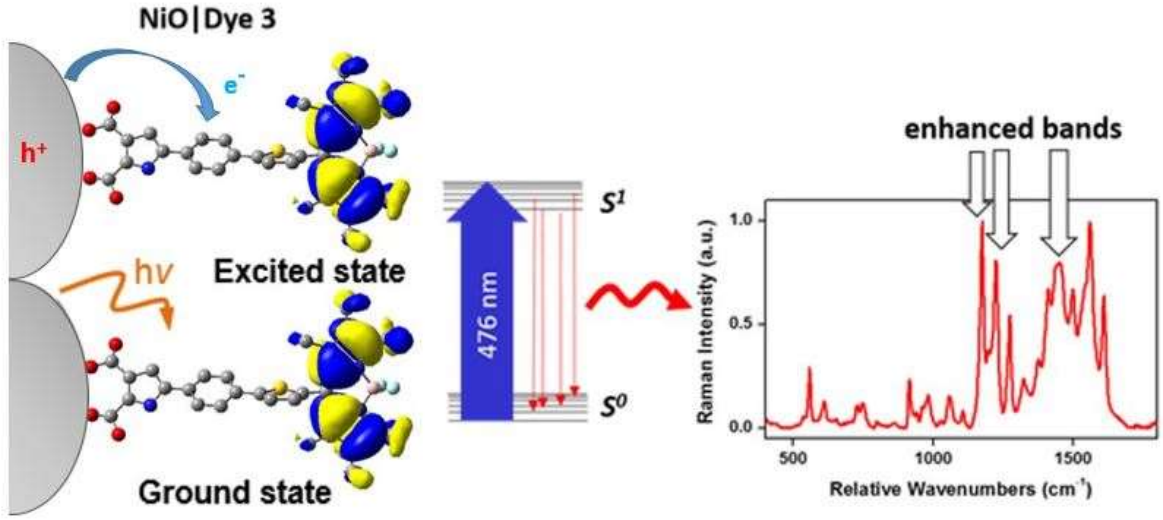

Introduction

Dye-sensitized nickel oxide (NiO) photocathodes offer an opportunity to harness solar energy cheaply and sustainably, either as part of a p-type dye-sensitized solar cell (p-DSC), or as part of a tandem dye-sensitized solar cell. In 1999 He *et al.* first introduced dye-sensitized NiO photocathodes for use in p-DSCs.[1] Then in 2000 the same authors reported the first tandem dye-sensitized solar cell, with a NiO photocathode and a titanium dioxide photoanode.[2] In these devices when the dye adsorbed onto the NiO surface is photo-excited, electron transfer from the NiO valence band to the dye occurs.[3,4] This process produces an intermediate charge-separated state, with a hole at the NiO surface and the negative charge localised on the reduced dye molecule. The photo-reduced dye can then reduce a redox mediator, which transports the electrons to an anode or photoanode. Reduction of the holes at the NiO surface by the photo-

reduced dye is a competing process, known as recombination.[5] Preventing this recombination is required to increase the efficiency of NiO solar cells.[6]

Push-pull dyes have been specifically developed to reduce recombination in NiO solar cells, by increasing the distance between the positive at the semiconductor surface and the negative charge localised on the photo-reduced dye to generate a stable charge-separated state.[4,7,8] These dyes are characteristically made-up of four parts: 1) an anchoring group which attaches the 2) electron donating group to the NiO, 3) a conjugated linker group that increases the distance between the attached 4) electron acceptor group and the NiO surface. Most successful push-pull dyes, such as **P1** (Figure 1) are based around a triphenylamine electron donating group anchored to NiO by a single carboxylate group. Bräutigam *et al*. have used rR spectroscopy to demonstrate the instability of dyes anchored to semiconductor surfaces with the traditional carboxylated bipyridyl Ru complexes in the presence of water.[9] The most efficient dye in NiO solar cells has a triphenylamine donor functionalised with two carboxylic acid anchoring groups to combat this instability.[10,11,12] Ji *et al.* designed a series of dyes which combined this double anchoring motif with the maleonitrile acceptor of **P1**.[13] In this series the linker group was varied between phenyl, thiophene and EDOT. The dye incorporating the thiophene linker (**O2** in Figure 1) out-performed the dye with the phenyl linker (**O6**). In a separate study, however, Qin *et al.* reported an improvement in performance when phenyl was used as the linker (**P4**) compared to thiophene (**P1**) in their system with a single anchoring group.[14]

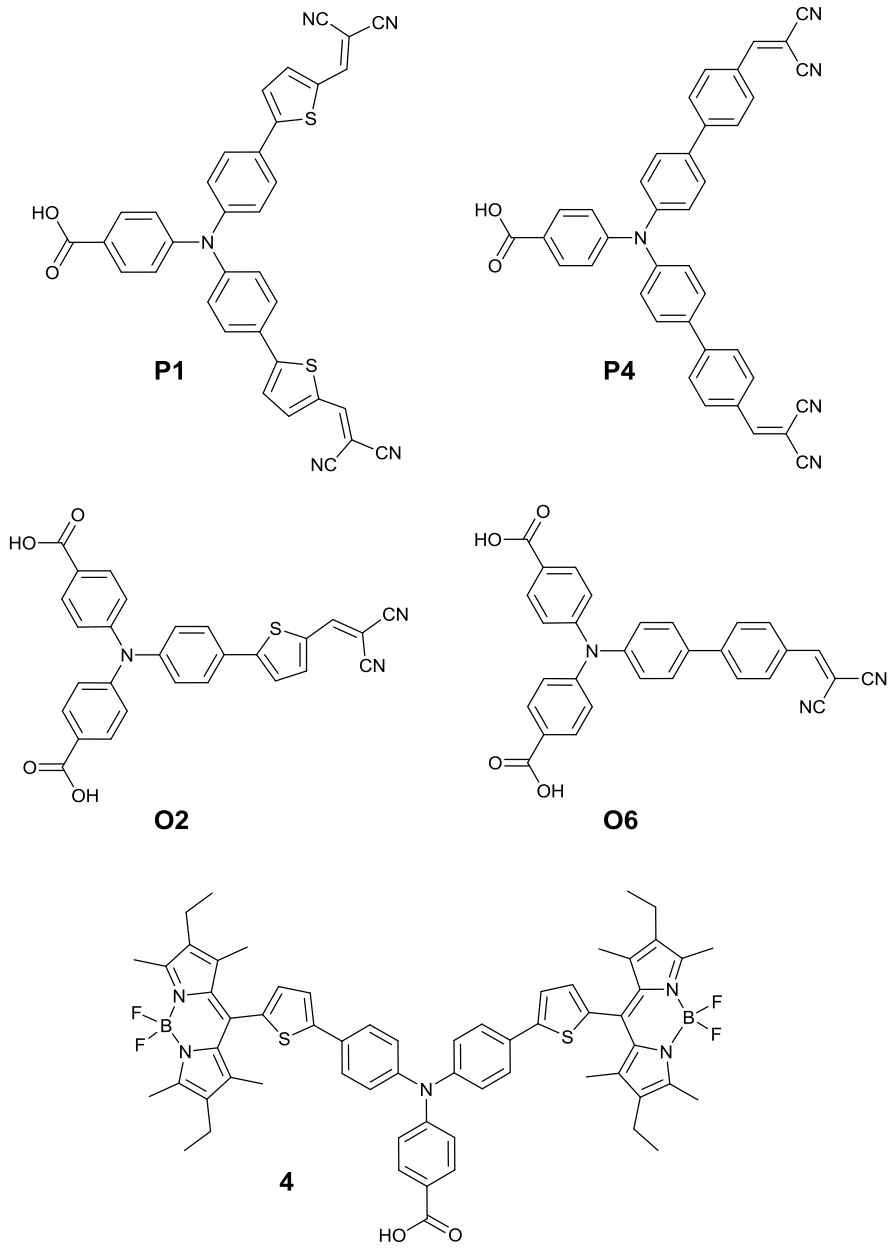

Figure 1. Structures of the dyes **P1** and **P4** reported by Qin *et al.*[14]and **O2** and **O6** reported by Ji *et al.*[13] and **4** reported by Lefebvre *et al.*[8]

Three push-pull dyes, **1**-**3**, incorporating a novel doubly anchored pyrrole donor group were designed, synthesised and evaluated a potential p-type dyes for solar cells (Figure 2). The pyrrole was prepared via nucleophilic catalysis using the previously reported method by Ngwerume *et al.*[15] We have varied the linker group in dyes **2** (diphenyl) and **3** (thiophene) to

compare the effects of the linker in the presence of the pyrrole anchoring moiety on the device performance and electronic properties. Dye **1** has been functionalised with a maleonitrile acceptor, allowing a direct comparison to **P1** and other triphenylamine-based dyes. Dyes **2** and **3** contain a boron-dipyrromethene (bodipy) group, which in dye **4** doubled the molar absorption coefficient compared to **P1**.[8] The photoinduced charge-separated state formed with **4**-sensitized NiO was previously shown to be three orders of magnitude longer compared to **P1**/NiO. This is possibly due to electronic decoupling of the LUMO from the triphenylamine/thiophene donor motif because of the steric demand of the methyl subsitutents on the dipyrromethene (see Figure 1).[8] Despite the better optoelectronic properties of **4**, the IPCE of the corresponding p-DSSC was only 28% compared to 64% for **P1**.[8,16]

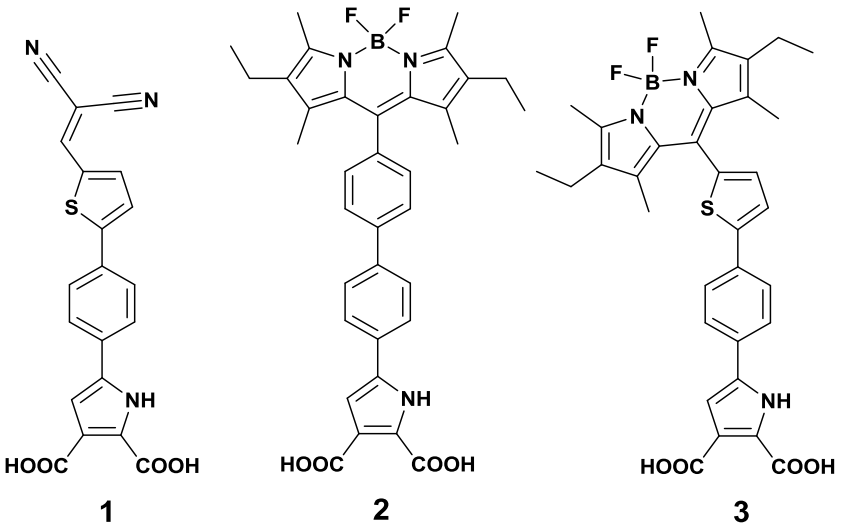

Figure 2. Structures of the dyes **1-3** used in this study.

Resonance Raman (rR) spectroscopy is commonly used for studying photoexcited metal-ligand charge transfer states of transition metal complexes.[17] It has been used to evaluate the coordination mode of ligands in ruthenium complexes such as the benchmark dye N719 and its interaction with a TiO_2 substrate.[18] Loppnow *et al.* used rR to probe the excited state metal-to-ligand charge transfer dynamics of N719 adsorbed on TiO_2.[19] More recently, rR

spectroscopy has also been used to map the distribution of a ruthenium dye adsorbed onto Ni and investigate the desorption kinetics.[9] Exciting a molecule at an electronic resonance enhances Raman bands of vibrational modes associated with the resulting optical transition. This indicates the bonds around which, in the excited electronic state, the electron density is more localised.[17] We have applied this principle to experimentally investigate the electron density distribution of the charge-separated states of a series of organic dyes adsorbed onto a NiO surface.

Herein we report how rR spectroscopy was used to investigate the electron density distribution of the previously reported dyes (**P1** and **4**) and the new pyrrole dyes (**1**-**3**), anchored to NiO, upon excitation with visible light. Dyes **1**-**3** were also incorporated into p-type dye-sensitized solar cells and the performances have been compared in the context of the results from the spectroscopic experiments.

Experimental

All reagents and solvents (analytical grade) were purchased from Sigma-Aldrich or Fisher Scientific and used without further purification unless stated. Dichloromethane was dried over calcium hydride and distilled under argon. Methanol was dried over magnesium turnings and iodine and distilled under argon. Silica gel 60 was purchased from Sigma-Aldrich. **P1** was synthesised using the method reported by Qin *et al.*,[7] **4** was prepared according to Lefebvre *et al.*[8] and dimethyl 5-(4-bromophenyl)-1H-pyrrole-2,3-dicarboxylate was synthesised using the method reported by Ngwerume *et al.*[15] Products were characterized by ^{1}H NMR and ^{13}C NMR using a Bruker 300 MHz (DPX300) or 400 (AV3400, DPX400, AV400) MHz spectrometer; chemical shifts (δ) are reported in parts per million (ppm) from low to high field and referenced to residual non-deuterated solvent (δ = 7.29 ppm for chloroform). Standard abbreviations indicating multiplicity are used as follows: s = singlet; d = doublet; t = triplet; m = multiplet.

High resolution mass spectrometry (HRMS) was carried out on a high-throughput MS system, based on a Bruker MicroTOF (Time of Flight) mass spectrometer using ElectroSpray Ionisation (ESI). Ultraviolet-visible absorption measurements were carried out using a Perkin Elmer Lambda 25 UV-Vis Spectrometer for samples in solution and a Jasco V-530 spectrometer for NiO films. Emission measurements were recorded using an Edinburgh Instruments FL900 fluorescence spectrometer.

2,3-Di(methylester)-pyrrole-5-phenyl-4-phenyl carboxaldehyde

Dimethyl 5-(4-bromophenyl)-1H-pyrrole-2,3-dicarboxylate (73 mg, 2.16×10^{-4} mol), 4-formylphenylboronic acid (60 mg, 2.59×10^{-4} mol, 1.2 equiv.), bis-triphenylphosphinepalladium(II) chloride (12.6 mg, 1.80×10^{-5} mol, 0.08 equiv.) and sodium carbonate (33.7 mg, 3.18×10^{-4} mol, 1.5 equiv.) were loaded in a Schlenk tube and purged with three vacuum/nitrogen cycles. H_2O (0.5 mL) and then 1,2-dimethoxyethane (2.5 mL) were added and the mixture was heated to 90 °C overnight under nitrogen. After cooling, H_2O (3 mL) was added and the mixture was acidified with diluted 0.1 M HCl until slightly acidic pH. The organic phase was extracted with EtOAc (3×5 mL), dried over $MgSO_4$ and the solvent was removed under reduced pressure. The residue was purified by silica gel column chromatography with a gradient of MeOH in CH_2Cl_2 as eluent to afford 2,3-di(methylester)-pyrrole-5-phenyl-4-phenyl carboxaldehyde (58 mg, 74%) as a white solid.

^{1}H NMR ($CDCl_3$, 400 MHz, 25 °C): δ 10.10 (s, 1H, H_{CHO}), 9.65 (br s, 1H, $H_{NH\ pyrrole}$), 8.01 (d, J = 8.4 Hz, 2H, H_{Ar}), 7.81 (d, J = 8.3 Hz, 2H, H_{Ar}), 7.75 (d, J = 8.6 Hz, 2H, H_{Ar}), 7.70 (d, J = 8.6 Hz, 2H, H_{Ar}), 7.04 (d, J = 3.2 Hz, 1H, $H_{pyrrole}$), 3.98 (s, 3H, H_{CH3}), 3.94 (s, 3H, H_{CH3}) ppm.

^{13}C NMR ($CDCl_3$, 100 MHz, 25 °C): δ 191.9, 164.3, 160.7, 146.1, 139.6, 135.6, 134.1, 130.5, 130.4, 128.3, 127.6, 125.5, 123.3, 121.8, 111.3, 52.5, 52.1 ppm.

MS (ESI$^+$): calcd. for $C_{19}H_{16}NO_5S$: 370.074, found: 370.076 ($[M+H]^+$).

calcd. for $C_{19}H_{15}NNaO_5S$: 392.056, found: 392.056 ($[M+Na]^+$).

MS (ESI$^-$): calcd. for $C_{19}H_{14}NO_5S$: 368.060, found: 368.061 ($[M-H]^-$).

2,3-Di(methylester)-pyrrole-5-phenyl-4-thienyl carboxaldehyde

Dimethyl 5-(4-bromophenyl)-1H-pyrrole-2,3-dicarboxylate (52 mg, 1.54×10^{-4} mol), 5-formyl-2-thienylboronic acid (36 mg, 2.31×10^{-4} mol, 1.5 equiv.), bis-triphenylphosphinepalladium(II) chloride (9 mg, 1.28×10^{-5} mol, 0.08 equiv.) and sodium carbonate (24 mg, 2.26×10^{-3} mol, 1.5 equiv.) were loaded in a Schlenk tube and purged with three vacuum/nitrogen cycles. H_2O (0.5 mL) and then 1,2-dimethoxyethane (3 mL) were added and the mixture was heated to 90 °C overnight under nitrogen. After cooling, the mixture was filtered and the filtrate acidified with diluted 0.1 M HCl until slightly acidic pH. The organic phase was extracted with EtOAc (3×10 mL), dried over $MgSO_4$ and the solvent was removed under reduced pressure to afford 2,3-di(carboxylic acid)-pyrrole-5-phenyl-4-phenyl carboxaldehyde (14 mg, 63%) as a white solid.

^{1}H NMR ($CDCl_3$, 400 MHz, 25 °C): δ 9.94 (s, 1H, H_{CHO}), 9.68 (br s, 1H, $H_{NH\ pyrrole}$), 7.79 (d, J = 4.0 Hz, 1H, $H_{thiophene}$), 7.76 (d, J = 8.4 Hz, 2H, H_{Ar}), 7.65 (d, J = 8.4 Hz, 2H, H_{Ar}), 7.48 (d, J = 4.0 Hz, 1H, $H_{thiophene}$), 7.03 (d, J = 3.0 Hz, 1H, $H_{pyrrole}$), 3.98 (s, 3H, H_{CH3}), 3.94 (s, 3H, H_{CH3}) ppm.

^{13}C NMR ($CDCl_3$, 100 MHz, 25 °C): δ 182.9, 164.2, 160.7, 153.2, 142.9, 137.5, 133.8, 133.0, 131.1, 127.3, 125.5, 124.5, 123.4, 121.8, 111.5, 52.5, 52.2 ppm.

MS (ESI$^+$): calcd. for $C_{19}H_{16}NO_5S$: 370.075, found: 370.072 ($[M+H]^+$).

calcd. for $C_{19}H_{15}NNaO_5S$: 392.057, found: 392.056 ($[M+Na]^+$).

MS (ESI$^-$): calcd. for $C_{19}H_{14}NO_5S$: 368.059, found: 368.060 ($[M-H]^-$).

2,3-Di(carboxylic acid)-pyrrole-5-phenyl-4-thienyl carboxaldehyde

To a suspension of dimethyl 5-(4-(5-formylthiophen-2-yl)phenyl)-1H-pyrrole-2,3-dicarboxylate (58 mg, 1.57 x 10^{-4} mol) in MeOH (20 mL) was added NaOH (150 mg, 3.75 x 10^{-3} mol, 24 equiv.) in water (20 mL) and the orange solution formed was heated at reflux for 12 h. After cooling to room temperature the solution was neutralised using 0.1 M HCl and extracted with ethyl acetate (4 x 50 mL). The combined organic layers were washed with brine (2 x 50 mL), dried over MgSO4, filtered and solvent was removed under reduced pressure to afford 5-(4-(5-formylthiophen-2-yl)phenyl)-1H-pyrrole-2,3-dicarboxylic acid (43 mg, 80%) as a yellow solid, which was used without further purification.

^{1}H NMR (DMSO-d^{6}, 300 MHz, 25 °C): δ 12.83 (br s, 1H), 9.91 (s, 1H), 8.04 (m, 3H), 7.83 (d, *J* = 9.1 Hz, 2H), 7.81 (d, *J* = 4.2 Hz, 1H), 7.22 (d, *J* = 2.8 Hz, 1H) ppm.

^{13}C NMR (DMSO-d^{6}, 75 MHz, 25 °C): δ 184.5, 169.0, 161.3, 152.5, 142.4, 139.7, 135.1, 132.2, 131.5, 127.0, 126.9, 126.8, 125.9, 119.9, 112.2 ppm.

MS (ESI^{-}): calcd. for $C_{17}H_{10}NO_5S$: 340.0285, found: 340.0287 ([M-H]$^{-}$).

Dye 1

2,3-Di(carboxylic acid)-pyrrole-5-phenyl-4-phenyl carboxaldehyde (22.1 mg, 6.47×10^{-5} mol) and malononitrile (4.5 mg, 6.81×10^{-5} mol, 1.05 equiv.) were dissolved in DMSO (5 mL). Et_3N (4 drops) were added and the mixture was stirred overnight at room temperature. CH_2Cl_2 (15 mL) was added to the solution and the precipitate was filtered, washed with CH_2Cl_2 and dried under reduced pressure to afford dye **1** (8.5 mg, 34%) as a brown solid.

^{1}H NMR (CD_3OD, 400 MHz, 25 °C): δ 7.80 (s, 1H, H_{vinyl}), 7.78 (d, *J* = 8.3 Hz, 2H, H_{Ar}), 7.75 (d, *J* = 8.3 Hz, 2H, H_{Ar}), 7.48 (d, *J* = 3.6 Hz, 1H, $H_{thiophene}$), 7.42 (d, *J* = 3.6 Hz, 1H, $H_{thiophene}$), 7.08 (s, 1H, $H_{pyrrole}$) ppm.

HRMS (TOF-ESI$^-$): calcd. for $C_{20}H_{10}N_3O_4S$: 388.0398, found: 388.0376 ($[M-H]^-$).

UV/Vis (DMSO): λ (ε, L mol^{-1} cm^{-1}) = 354 (17750).

2,3-Di(methylester)-pyrrole-5-phenyl-4-phenyl-(2,6-diethyl-4,4-difluoro-1,3,5,7 tetramethyl-4-bora-3a,4a-diaza-s-indecene), $\mathbf{2_{Me}}$

2,3-Di(methylester)-pyrrole-5-phenyl-4-phenyl carboxaldehyde (25 mg, 6.88×10^{-5} mol) was dissolved in dry CH_2Cl_2 (1.1 mL) in a Schlenk tube and purged with three vacuum/nitrogen cycles. 2,4-Dimethyl-3-ethylpyrrole (30 µL, 2.22×10^{-4} mol, 3.2 equiv.) and trifluoroacetic acid (1 drop) were added. The mixture was stirred for five hours under nitrogen. *p*-Chloranil (16.9 mg, 6.87×10^{-5} mol, 1.0 equiv.) was added under a flux of nitrogen and the mixture was stirred under nitrogen for 1 h. Diisopropylethylamine (100 µL, 5.74×10^{-4} mol, 8.3 equiv.) was added and the mixture was stirred under nitrogen for 15 min. Boron trifluoride etherate (100 µL, 8.10×10^{-4} mol, 11.8 equiv.) was added and the mixture was stirred under nitrogen for 1 h. CH_2Cl_2 (5 mL) was added to the mixture and the organic layer was washed with H_2O (4×3 mL), dried over $MgSO_4$ and removed under reduced pressure. The residue was purified by silica gel column chromatography with a CH_2Cl_2 / MeOH mixture (*v/v* 99/1). Crystallisation from CH_2Cl_2 with addition of pentane afforded $\mathbf{2_{Me}}$ (20.3 mg, 47%) as a red solid.

^{1}H NMR ($CDCl_3$, 400 MHz, 25 °C): δ 9.64 (s br, 1H, $H_{NH\ pyrrole}$), 7.80 (d, *J* = 8.3 Hz, 4H, H_{Ph}), 7.71 (d, *J* = 8.3 Hz, 2H, H_{Ph}), 7.41 (d, *J* = 8.3 Hz, 2H, H_{Ph}), 7.04 (d, *J* = 2.9 Hz, 1H, $H_{pyrrole}$), 3.99 (s, 3H, H_{COOCH3}), 3.95 (s, 3H, H_{COOCH3}), 2.57 (s, 6H, H_{Me}), 2.34 (q, *J* = 7.5 Hz, 4H, H_{CH2CH3}), 1.38 (s, 6H, H_{Me}), 1.02 (t, *J* = 7.5 Hz, 6H, H_{CH2CH3}) ppm.

^{13}C NMR ($CDCl_3$, 100 MHz, 25 °C): δ 164.3, 160.7, 154.8, 145.4, 138.7, 135.6, 134.2, 133.7, 133.4, 131.8, 129.8, 129.3, 126.5, 125.4, 123.7, 123.1, 121.8, 111.1, 76.8, 52.5, 52.1, 17.3, 14.7, 12.7, 11.4 ppm.

HRMS (TOF-ESI$^+$): calcd. for $C_{37}H_{38}BF_2N_3NaO_4$: 660.2822, found: 660.2840 ($[M+Na]^+$).

UV/Vis (CH_2Cl_2): λ (ε, L mol^{-1} cm^{-1}) = 324 (29 500), 407 (sh, 5000), 499 (sh, 18 000), 526 (52 000) nm.
(CH_3CN): λ (ε, L mol^{-1} cm^{-1}) = 363 (60 000), 411 (sh, 16 200), 512 (sh, 40 000), 536 (112 000) nm.

Dye 2

2,3-Di(methylester)-pyrrole-5-phenyl-4-phenylboradiazaindecene (**2$_{Me}$**, 10 mg, 1.57×10^{-5} mol) was dissolved in dry MeCN (20 mL) in a Schlenk tube purged with three vacuum/nitrogen cycles. Bromotrimethylsilane (0.12 mL, 62.74×10^{-5} mol, 40 equiv.) was added and the mixture was stirred at reflux for 7 d. Acetonitrile was removed under reduced pressure and the crude residue was stirred in MeOH (10 mL) overnight. MeOH was removed under reduced pressure and the residue was dissolved in dry CH_2Cl_2 (10 mL) followed by the addition of diisopropylethylamine (29 µL, 1.66×10^{-4} mol, 10.5 equiv.), which was stirred under nitrogen for 15 min. Boron trifluoride etherate (35 µL, 2.84×10^{-4} mol, 18 equiv.) was added and the mixture was stirred under nitrogen for 1 h. The organic layer was washed with H_2O (3×10 mL), dried over $MgSO_4$ and removed under reduced pressure. The residue was purified by size exclusion chromatography on Sephadex LH-20 with a MeOH eluent. Crystallisation from CH_2Cl_2 with addition of pentane afforded dye **2** (5.9 mg, 62%) as a red solid.

^{1}H NMR (CD_3OD, 400 MHz, 25 °C): δ 7.96 (d, *J* = 8.5 Hz, 2H, H_{Ph}), 7.90 (d, *J* = 8.2 Hz, 2H, H_{Ph}), 7.86 (m, 2H), 7.43 (d, *J* = 8 Hz, 2H, H_{Ph}), 7.09 (d, *J* = 3.9 Hz, 1H, $H_{pyrrole}$), 2.49 (s, 6H, H_{Me}), 2.36 (q, *J* = 7.6 Hz, 4H, $H_{CH_2CH_3}$), 1.43 (s, 6H, H_{Me}), 1.01 (t, *J* = 7.6 Hz, 6H, $H_{CH_2CH_3}$) ppm.

HRMS (TOF-ESI$^-$): calcd. for $C_{35}H_{33}BF_2N_3O_4$: 608.254, found: 608.243 ($[M-H]^-$)

UV/Vis (CH_2Cl_2): λ (relative intensity (%)) = 512 (41), 536 (100) nm.

(CH_3CN): λ (relative intensity (%)) = 499 (40), 526 (100) nm.

2,3-Di(methylester)-pyrrole-5-phenyl-4-thienyl-(2,6-diethyl-4,4-difluoro-1,3,5,7 tetramethyl-4-bora-3a,4a-diaza-s-indecene), 3_{Me}

2,3-Di(methylester)-pyrrole-5-phenyl-4-thienyl carboxaldehyde (25 mg, 6.77×10^{-5} mol) was dissolved in dry CH_2Cl_2 (1.1 mL) in a Schlenk tube and purged with three vacuum/nitrogen cycles. 2,4-Dimethyl-3-ethylpyrrole (28 µL, 2.07×10^{-4} mol, 3.1 equiv.) and then trifluoroacetic acid (1 drop) were added to the solution. The mixture was stirred for 5 h under nitrogen. *p*-Chloranil (16.6 mg, 6.75×10^{-5} mol, 1.0 equiv.) was added under a flux of nitrogen and the mixture was stirred under nitrogen for 1 h. Diisopropylethylamine (71 µL, 4.08×10^{-4} mol, 6.0 equiv.) was added and the mixture was stirred under nitrogen for 15 min. Finally, boron trifluoride etherate (84 µL, 6.81×10^{-4} mol, 10.1 equiv.) was added and the mixture was stirred under nitrogen for 1 h. CH_2Cl_2 (10 mL) was added to the mixture and the organic layer was washed with H_2O (4×5 mL), dried over $MgSO_4$ and removed under reduced pressure. The residue was purified by silica gel column chromatography with a CH_2Cl_2 / MeOH gradient mixture (*v/v* 99/1). Crystallisation from CH_2Cl_2 with addition of pentane afforded **3_{Me}** (27 mg, 63%) as a red solid.

^{1}H NMR ($CDCl_3$, 400 MHz, 25 °C): δ 9.56 (s br, 1H, $H_{NH\ pyrrole}$), 7.73 (d, *J* = 8.3 Hz, 2H, H_{Ph}), 7.62 (d, *J* = 8.3 Hz, 2H, H_{Ph}), 7.41 (d, *J* = 3.6 Hz, 1H, $H_{thiophene}$), 7.01 (d, *J* = 3.0 Hz, 1H, $H_{pyrrole}$), 7.00 (d, *J* = 3.6 Hz, 1H, $H_{thiophene}$), 3.99 (s, 3H, H_{COOCH3}), 3.94 (s, 3H, H_{COOCH3}), 2.57 (s, 6H, H_{Me}), 2.36 (q, *J* = 7.5Hz, 4H, H_{CH2CH3}), 1.66 (s, 6H, H_{Me}), 1.04 (t, *J* = 7.5Hz, 6H, H_{CH2CH3}) ppm.

^{13}C NMR ($CDCl_3$, 100 MHz, 25 °C): δ 164.3, 160.7, 154.0, 140.5, 140.1, 138.5, 135.4, 134.33, 133.0, 130.9, 129.7, 129.2, 127.9, 127.5, 125.4, 123.1, 121.8, 111.1, 52.5, 52.1, 17.3, 14.8, 12.7, 12.1 ppm.

HRMS (TOF-ESI$^+$): calcd. for $C_{35}H_{36}BF_2N_3NaO_4S$: 666.2392, found: 666.2386 ($[M+Na]^+$).

UV/Vis (CH_2Cl_2): λ (ε, L mol^{-1} cm^{-1}) = 341 (33 000), 411 (sh, 9 300), 497 (sh, 19 000), 541 (51 500) nm.
(CH_3CN): λ (ε, L mol^{-1} cm^{-1}) = 363 (60 000), 411 (sh, 16 200), 512 (sh, 40 000), 536 (112 000) nm.

Dye 3

2,3-Di(methylester)-pyrrole-5-phenyl-4-thienylboradiazaindecene (**3$_{Me}$**, 11 mg, 2.02×10^{-5} mol) was dissolved in dry MeCN (20 mL) in a Schlenk tube and purged with three vacuum/nitrogen cycles. Bromotrimethylsilane (0.16 mL, 80.80×10^{-5} mol, 40 equiv.) was added via syringe and the mixture was stirred at reflux for 7 d. MeCN was removed under reduced pressure and the crude residue was stirred in MeOH (10 mL) overnight. MeOH was removed under reduced pressure and the residue dissolved in dry CH_2Cl_2 (10 mL) followed by the addition of diisopropylethylamine (29 µL, 1.66×10^{-4} mol, 8.2 equiv.), which was stirred under nitrogen for 15 min. Boron trifluoride etherate (35 µL, 2.84×10^{-4} mol, 14 equiv.) was

added and the mixture was stirred under nitrogen for 1 h. The organic layer was washed with H_2O (3×10 mL), dried over $MgSO_4$ and removed under reduced pressure. The residue was purified by size exclusion chromatography on Sephadex LH-20 with a MeOH eluent. Crystallisation from CH_2Cl_2 with addition of pentane afforded dye **3** (7.5 mg, 71%) as a red solid.

^{1}H NMR (CD_3OD, 400 MHz, 25 °C): δ 7.80 (4H, m, H_{Ph}), 7.58 (d, *J* = 3.7 Hz, 1H, $H_{thiophene}$), 7.11 (m, 2H, $H_{pyrrole/}$ $H_{thiophene}$), 2.52 (s, 6H, H_{Me}), 2.42 (q, *J* = 7.5Hz, 4H, H_{CH2CH3}), 1.73 (s, 6H, H_{Me}), 1.05 (t, *J* = 7.5Hz, 6H, H_{CH2CH3}) ppm.

HRMS (TOF-ESI$^-$): calcd. for $C_{33}H_{31}BF_2N_3O_4S$: 614.210, found: 614.218 ($[M-H]^-$)

UV/Vis (CH_2Cl_2): λ (relative intensity (%)) = 324 (80), 407 (23), 499 (45), 526 (100) nm.
(CH_3CN): λ (relative intensity (%)) = 411 (23), 512 (42), 536 (100) nm.

Preparation of Dyed NiO Surfaces for rR Measurements

Anhydrous $NiCl_2$ (1.00 g, 7.72 mmol) and templating polymer F-108 (1.00 g) were mixed with EtOH (6.00 mL) and ultra-pure H_2O (5.00 mL), then stirred overnight until all compounds were fully dissolved. The solution was left to settle and centrifuged to remove precipitates a few days prior to use. Microscope slides were heated to 450 ˚C, then a saturated solution of $NiCl_2$ in acetylacetone was sprayed on one side and the substrate was left to cool to room temperature. The$NiCl_2$/F-108 solution was applied by doctor-blading, using Scotch tape as a mask with a 1 cm diameter hole. The films were calcined at 450 ˚C for 30 min and once the surfaces had cooled to room temperature a second layer of NiO was added by repeating the masking, doctor-blading and heating steps. The films were then submerged in a solution of dye (approx. 0.3

mM) in CH_2Cl_2 or DMF for 2 days. Prior to each measurement the surfaces were rinsed with CH_2Cl_2 and UV-visible absorption spectra were measured using a Jasco V-530 spectrometer.

Resonance Raman Spectroscopy

A Labram HR800, Horiba Jobin Yvon micro-Raman setup was used, with a 600 lines per millimetre grating combined with an Olympus BX 41 microscope. A Coherent Innova 301C krypton-ion laser was used to deliver excitation wavelengths of 413 nm or 476 nm, which were focused on the sample using an Olympus 20× microscope objective lens to a spot size of about 1 μm. The laser power was 2.5 mW.

The spectra of the dyed NiO surfaces shown were obtained from the mean spectra of a quadratic map for each sample, with a 60 μm edge length and spectra integrated over 1 s for 10×10 points, as described by Bräutigam *et al.*[9] Any outlier values were removed from the dataset prior to calculating the mean spectra using Gnu R version 2.15.3 with the library "outliers".[20] Luminescence was seen in all the spectra, even for dye|NiO, and corrected *via* SNIP algorithm using the library "Peaks". UV-visible spectra of the dye|NiO samples were taken prior to each rR measurement.

Solar cells

NiO precursor solution was prepared by dissolving anhydrous $NiCl_2$ (1 g) and the tri-block co-polymer F108 (poly (ethylene glycol)-*block*-poly (propylene glycol)-*block*-poly (ethylene glycol)) (1 g) in ethanol (6 g) and ultrapure Milli-Q water (5 g). p-DSCs were made by spreading the precursor solution described above onto conducting glass substrates (Pilkington TEC15, sheet resistance 15 Ω/square) using Scotch tape as a spacer (0.2 cm^2 active area),

followed by sintering in an oven at 450 °C for 30 min. The NiO electrodes were soaked in a DMF solution of **1** or an acetonitrile solution of **2** or **3** (0.3 mM) for 16 h at room temperature. The dyed NiO electrode was assembled face-to-face with a platinized counter electrode (Pilkington TEC8, sheet resistance 8 Ω/square) using a 30 mm thick thermoplastic frame (Surlyn 1702, Dyesol). The electrolyte, containing LiI (1.0 M) and I_2 (0.5 M or 0.1 M) in acetonitrile, was introduced through a pre-drilled hole in the counter electrode, which was sealed afterwards. Current-voltage measurements were measured using an Ivium CompactStat potentiostat under AM1.5 simulated sunlight from an Oriel VeraSol-2 Class AA LED Solar Simulator. The light intensity (100 mW cm^{-2}) was calibrated against a certified reference cell (Newport). Incident photon-to-current conversion efficiencies were recorded using monochromatic light from the Oriel 300 W Xe lamp fitted with an AM1.5 filter, using a Cornerstone monochromator and calibrated against a certified reference Si photodiode.

Results and discussion

Synthesis

Dimethyl 5-(4-bromophenyl)-1H-pyrrole-2,3-dicarboxylate was synthesised as described previously.[15] The linker units were introduced by Suzuki-coupling reactions with 4-formylphenyl and 5-formyl-2-thienyl boronic acids with yields of 74% and 87% respectively. For dye **1** the anchor groups were first hydrolysed by refluxing in basic methanol followed by condensation of malononitrile. For dyes **2** and **3** the bodipy groups were introduced via a condensation reaction with 2,4-dimethyl-3-ethylpyrrole, oxidation with p-chloranil and subsequent coordination of boron trifluoride etherate. The anchoring groups were hydrolysed by refluxing with bromotrimethyl silane following workup with methanol. It was found that this step removed the boron fragment, resulting in formation of the dipyrromethene, which was subsequently coordinated following the same procedure as before.

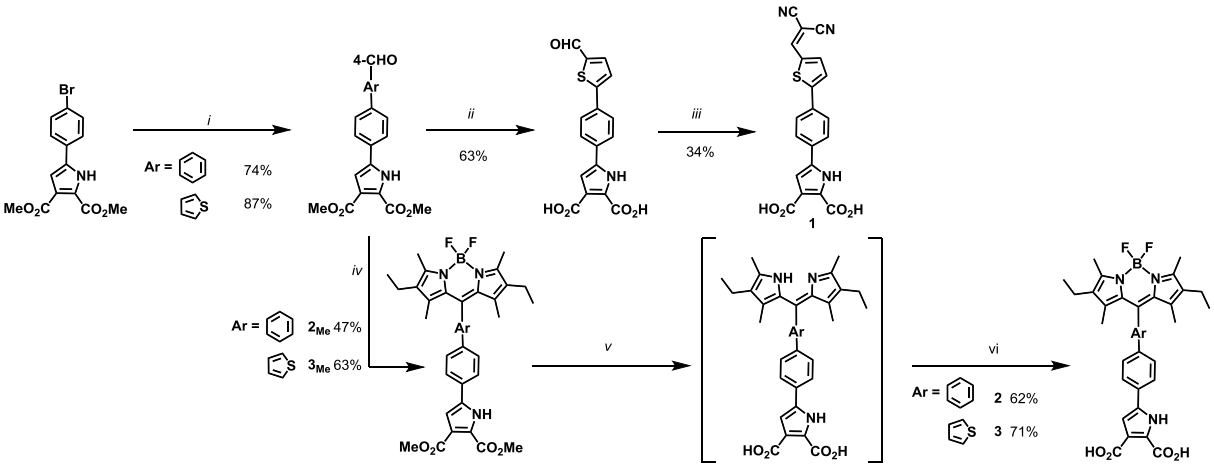

Scheme 1. Synthesis of dyes **1-3.** Reagents and conditions: (i) 5-formyl-2-thienylboronic acid or 4-formylphenylboronic acid, Na_2CO_3, $Pd(PPh_3)_2Cl_2$, H_2O, DME, 90 °C, 12 h; (ii) NaOH, MeOH, reflux, 12 h, 63%; (iii) Malononitrile, Et_3N, DMSO, rt, 12 h, 34%; (iv) a) 2,4-dimethyl-3-ethylpyrrole, trifluoroacetic acid, CH_2Cl_2, rt, 5 h; b) p-chloranil, rt, 1 h; c) $NEt(iPr)_2$, rt, 15 min; -d) $BF_3{\cdot}OEt_2$, rt, 1 h; (v); a) TMSBr, MeCN, reflux 7 d; b) MeOH, rt 12 h; (vi); a) $NEt(iPr)_2$, CH_2Cl_2, rt, 15 min; b) $BF_3{\cdot}OEt_2$, rt, 1 h.

UV-visible absorption and emission spectra

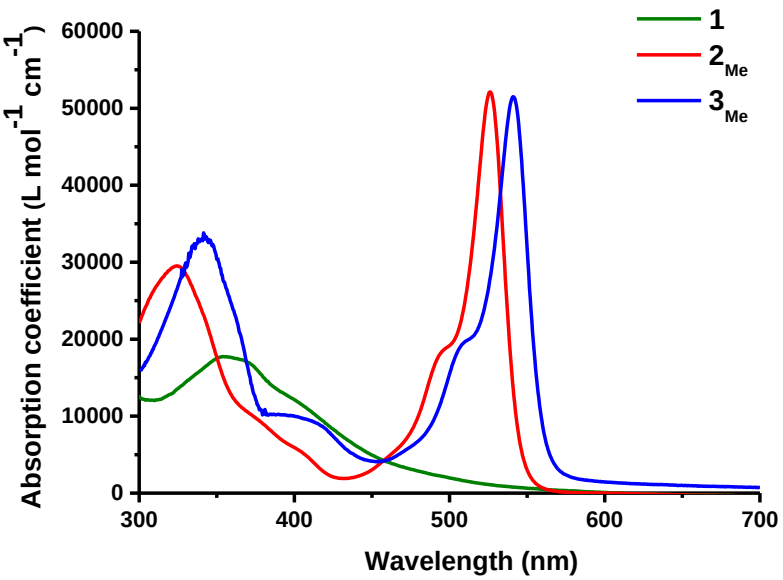

Figure 3a. Molar absorption coefficients of **1** (in DMSO)**, 2Me** and **3Me** (in dichloromethane)

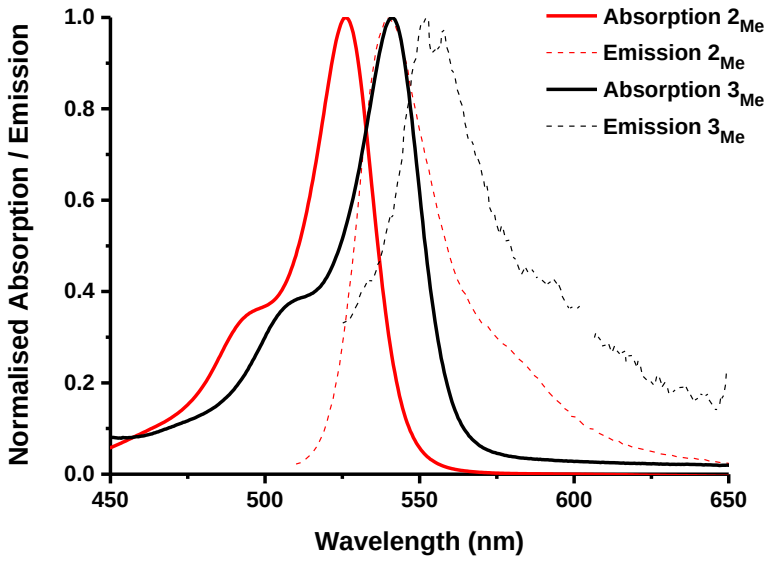

Figure 3b. Normalised absorption and emission spectra of **2Me** and **3Me** in dichloromethane.

Absorption and emission spectra of **1** and the methyl esters of the dyes, **2**Me and **3**Me, in solution are shown in Figure 3. The spectra of both **2Me** and **3Me** and the small Stokes shift are characteristic of bodipy derivatives. The spectra for **3Me** were red-shifted relative to **2Me** which implies that the electronic properties of the spacer affect the electronic properties of the electron

acceptor. The absorption spectrum of **1** has a maximum at higher energy than **2** and **3**, which overlapped with the absorption of the NiO when adsorbed onto the surface (See Figure S3 in the ESI). Organic push-pull dyes with a maleonitrile acceptor group, such as **P1**, usually have a much lower energy absorption with a maximum around 500 nm.[7]

Resonance Raman spectra

Unfortunately, the dyes were too emissive to measure the Raman or rR of the dyes in the absence of NiO. When adsorbed onto NiO the emission was (partially) quenched, which enabled rR spectra to be recorded. The bands which are enhanced in the rR spectra are related to molecular geometry changes arising from the change in the distribution of electron density in the excited state compared to the ground state. In all spectra, the absence of the carbonyl stretching mode band at 1791 cm^{-1} was noticeable, which can be attributed to successful adsorption of the dyes onto the NiO surface.

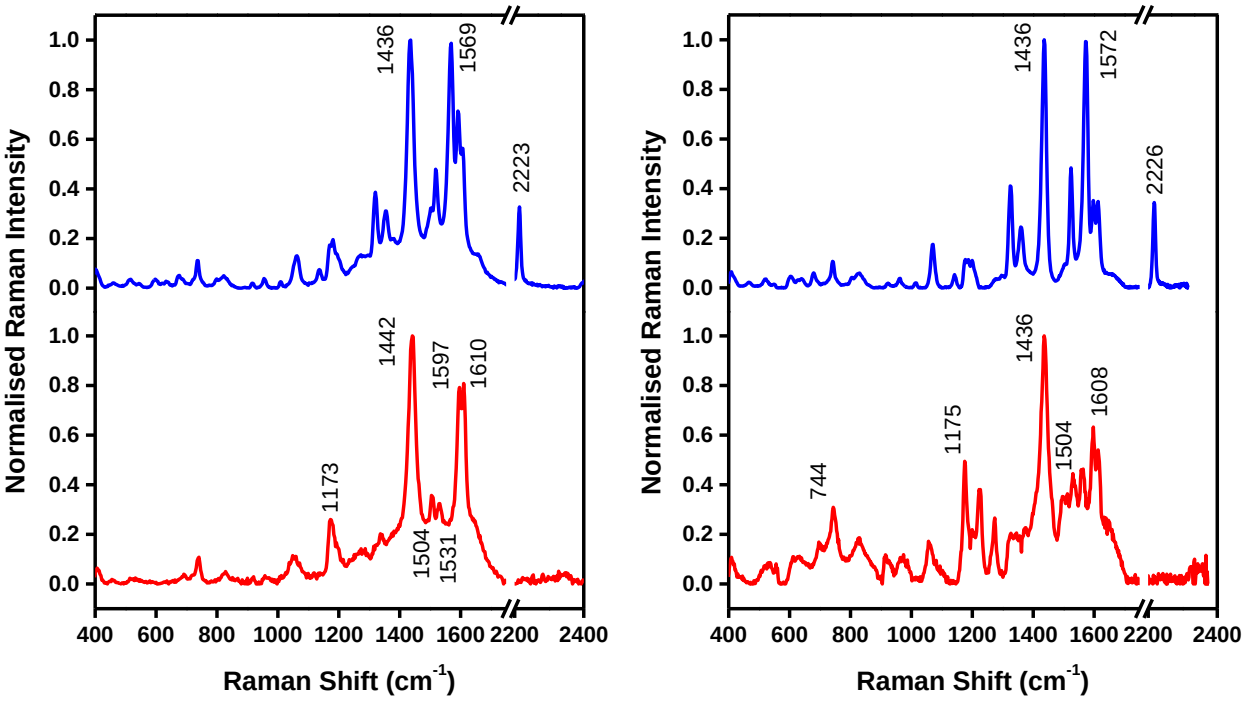

Figure 4. rR spectra of **P1**|NiO (blue) and **4**|NiO (red) excited at 413 nm (left), and 476 nm (right).

The rR spectra of the dyes|NiO are shown in Figure 4. An excitation wavelength of 476 nm was chosen to access the lowest energy singlet excitations, $S_0 \rightarrow S_1$ of each dye. In the rR spectra of both **P1**|NiO and **4**|NiO excited with 476 nm light, the most intense band is at 1436 cm^{-1}. This band is in the typical frequency range observed for the symmetric ring stretching modes of a thiophene group.[21–23] The bands at 1558 cm^{-1} correspond to the asymmetric stretch of the thiophene ring. Resonance enhanced bands at 1572 cm^{-1} for **P1**|NiO and 1608 and 1592 cm^{-1} for **4**|NiO are characteristic of C=C and C-C phenyl ring stretching.[24] The band at 2226 cm^{-1} in the rR spectrum of **P1**|NiO is due to the asymmetric nitrile stretching mode of one of the maleonitrile acceptors (Figure 4). Enhanced bands at 1530 and 1504 cm^{-1} are within the characteristic frequency range of dipyrrin.[23,25] Three bands between 1170-1300 cm^{-1} are consistent with the pyrrole and diene. A band at 1175 cm^{-1} is close in wavenumber to a band

reported at 1172 cm^{-1} for crystals of bodipy analogues by Badré *et al*.[26] These enhanced bands correspond with geometry changes during the photoexcitation.

Figure 4 also contains the rR spectra of **P1**|NiO and **4**|NiO recorded using an excitation wavelength of 413 nm. According to TDDFT calculations, at this wavelength the electronic transition for **P1** is still likely to be predominantly HOMO-LUMO and HOMO-LUMO+1 which is associated with a shift in electron density towards the thiophene and cyanovinyl moieties for both transitions.[4] Consistent with this, both rR spectra of **P1**|NiO in Figure 4 are similar. In contrast, the rR spectra for **4**|NiO in Figure 4 excited at 413 nm and at 476 nm are remarkably different. When **4**|NiO was excited at 413 nm, bands at 1610 cm^{-1} and 1442 cm^{-1}, which were respectively assigned to phenyl and thiophene ring stretching modes, were enhanced. Whereas the bands at 1531, 1504 and 1170-1300 cm^{-1} associated with the bodipy moiety were very weak or not enhanced. These results suggest that there are two electronic states accessible by photo-excitation for **4**, which is in agreement with the emission reported by Lefebvre *et al.*[8] In CH_3CN solution, **4** emits from the higher energy triphenyl amine moiety (λ_{max} = 475 nm) when excited at 406 nm, and the lower energy bodipy (λ_{max} = 560 nm) when excited at 488 nm. Lefebvre *et al.* also noted that emission from **4** is solvent dependent and in CH_2Cl_2 solution, **4** emits from the bodipy (λ_{max} = 560 nm) when excited at 406 nm.[8]

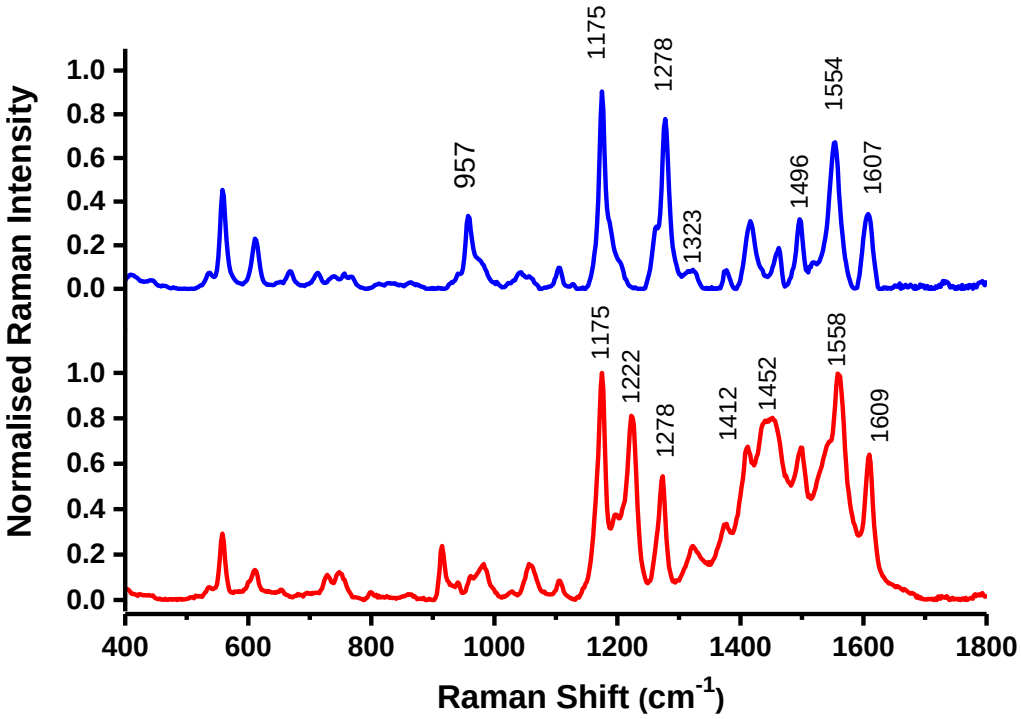

Figure 5. rR spectra of **2**|NiO (blue) and **3**|NiO (red) excited at 476 nm. The intensity of both spectra were normalised with respect to the common band at 1175 cm^{-1}.

The rR spectra of **2** and **3** adsorbed onto NiO (**2**|NiO, **3**|NiO) were taken at 476 nm excitation (Figure 5). The most intense band in both spectra was observed at 1175 cm^{-1}, which agrees with **4**|NiO and is consistent with a change in electron density at the bodipy. Both spectra have a less intense band, at 1607 cm^{-1} for **2**|NiO and at 1609 cm^{-1} for **3**|NiO, which has been assigned to the phenyl ring stretch consistent with our assignment in **4**|NiO. This is accompanied by a band at 1554 cm^{-1} in **2**|NiO and 1558 cm^{-1} in **3**|NiO, the latter is consistent with **4**|NiO.

In the spectrum for **2** another band at 957 cm^{-1} is enhanced. We have assigned the intense bands at 1278 cm^{-1} to the pyrrole group. For **3**, the enhanced band at *ca.* 1452 cm^{-1} is consistent with thiophene. A band at 1230 cm^{-1} is present in the rR spectrum of **3** but is absent in the spectrum of **2** and so we have also assigned this to vibrations associated with the thiophene bridge. The enhancement of bands corresponding to pyrrole and bodipy is consistent with photoinduced

charge-transfer rather than bodipy-localised π-π* transitions ($S_0 \rightarrow S_1$). This charge-transfer transition may be intramolecular (e.g. the $S_0 \rightarrow S_2$ transition for **3**) or from the NiO to the dye. As the UV-visible absorption spectra are sharp and not strongly solvent dependent (Figure S1 and S2), the experimentally observed emission quenching is consistent with photoinduced charge-transfer from NiO to the dye and suggests that the spectra in Figure 5 correspond to $NiO^{+}|dye^{-}$.

For comparison, the spectra of **2**|NiO and **3**|NiO were also recorded using 413 nm excitation (Figure 6). This wavelength corresponds to a higher energy transition compared to Figure 5. The most intense band of both the Raman spectra of **2** and **3** excited at 413 nm was observed at 1605 cm^{-1}. This vibrational mode, which has been assigned to a symmetric phenyl ring stretch, was also present in the spectra for **2** and **3** excited at 476 nm and in the spectra for **1** excited at 413 nm. As in Figure 5, a band was present in the region which is characteristic of the symmetric ring stretching mode of thiophene (1441 cm^{-1}) in the rR spectra of **3** but not **2**.[27] Therefore, the rR spectra of **2**|NiO and **3**|NiO and excited at 413 nm are consistent with changes in electron density on the anchor and linker.

Dye **1** cannot be excited resonantly at 476 nm, hence only 413 nm excitation was used (Figure 6). The most intense bands in the rR spectrum of **1** were found at 1455 and 1610 cm^{-1}. Previous spectroscopic studies of para-phenylthiophene copolymers have assigned bands around 1446 cm^{-1} to the symmetric ring stretching mode of the thiophene. This assignment is consistent with **1** since this band is also present in the rR spectra of **3** but not **2** (Figures 5 and 6).[27] The band at 2221 cm^{-1} is within the typical region for a CN stretch on the maleonitrile. The low intensity implies that the electron density on the maleonitrile acceptors is relatively unchanged on excitation. Instead, it appears that this transition leads to a change in electron density around the pyrrole donor group and the phenyl part of the linker. In a solar cell, the efficiency is usually higher for dyes that promote a shift in electron density away from the NiO surface, towards the

electron acceptor (and the electrolyte solution). The low intensity of the nitrile band in the rR spectrum is not consistent with this mechanism and implies that **1** may not promote charge-separation as effectively as **2** and **3**.

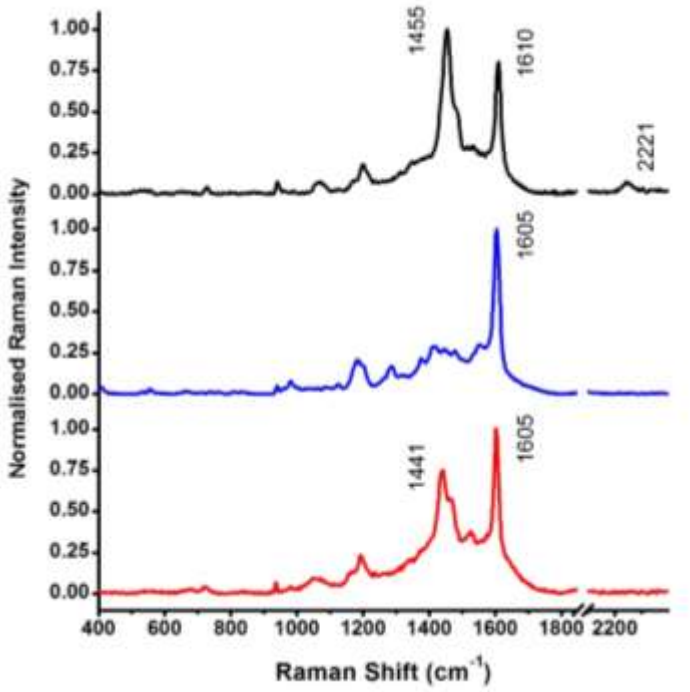

Figure 6. rR spectrum of **1**|NiO (black), **2**|NiO (blue) and **3**|NiO (red) excited at 413 nm. The intensities were normalised with respect to the most intense bands, which were at 1455 cm^{-1} for **1** and 1604 cm^{-1} for **2** and **3**.

Dye-sensitized solar cells

To investigate the performance of the dyes in a device they were adsorbed onto NiO electrodes and assembled into p-type DSCs, according to the method outlined in the experimental section. In order to obtain an absorbance above 1 (i.e. a light harvesting efficiency above 90%), four layers of NiO film were deposited on to the SnO_2:F coated glass substrate using the method described by Li *et al*.[16,28] The photocurrent - photovoltage curves of the p-type dye-sensitized solar cell (p-DSC) were measured under AM 1.5, 100 mW cm^{-2} conditions and the

characteristics are summarised in Table 2. The V_{OC} of NiO-based p-DSCs is typically low (*ca.* 100 mV) because of the small potential difference between the valence band edge in NiO and the redox potential of the electrolyte. The V_{OC} of the devices incorporating **1-3** was lower than typically generated in devices using triphenylamine-based dyes.[8,16,28,29] This is possibly due to an upward shift in the Fermi level due to increased recombination at the electrolyte/NiO interface or a difference in the dipole at the dye/NiO interface compared to triphenylamine containing dyes such as **P1**.[29] Both the J_{SC} and V_{OC} were better for the device incorporating dye **3** compared to dye **2** giving rise to a higher efficiency of 0.023% for **3** compared to 0.009% for **2**. The low fill factors are typical for NiO DSCs.[6] The incident photon to current conversion efficiency (IPCE) spectra are provided in Figure 7 and resemble the profile of the absorption spectra in Figure 3. In all three spectra there is a contribution at 400 – 450 nm which is likely to contain a contribution from photolysis of triiodide as well as from photoexcitation of the dyes.[30] Since the maximum absorption for **1** overlaps with the absorption spectrum of triiodide and the absorption coefficient is relatively low compared to the bodipy dyes, it is unsurprising that this dye produced the least photocurrent overall. The maximum IPCE of the solar cell incorporating **3** was twice as high as that of the device incorporating **2,** which is consistent with the higher short-circuit photocurrent density under simulated sunlight. We attribute this improvement to the thiophene being a better electronic linker between the anchoring group and the bodipy acceptor, as evidenced from the rR experiments. These results are consistent with the previous results reported by Ji *et al.* for triphenyl amine-based dyes with two carboxylic acid anchoring groups.

Table 2. Photovoltaic performance of p-DSCs based on NiO with the different dyes.

Dye	Absorbance	J_{SC}^{a} / mA cm^{-2}	V_{OC}^{b} / mV	FF^{c} / %	η^{d} / %	$IPCE^{e}$ / %
1	1.05	0.31	41	31	0.004	10
2	1.25	0.53	53	30	0.009	5
3	1.50	1.17	61	32	0.023	11

(a) *J*sc is the short-circuit current density at the $V = 0$ intercept, b) V_{OC} is the open-circuit voltage at the $J = 0$ intercept, c) *FF* is the device fill factor; d) η is the power conversion efficiency, e) IPCE is the monochromatic incident photon-to-current conversion efficiency.

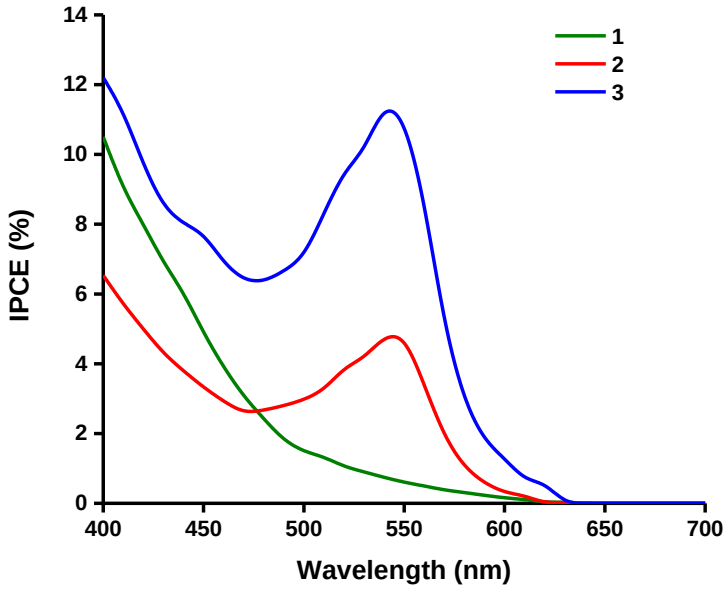

Figure 7. IPCE spectra for NiO DSCs with **1**, **2** and **3.**

Conclusions

Three new dyes with a novel dicarboxylic acid-pyrrole anchoring group were designed, synthesised and their solar cell performances were evaluated. These anchoring groups open up new opportunities for the development of p-type dye structures with controlled geometry and electronic properties. However, the dyes did not perform as well as dyes containing triphenylamine donors and bodipy or maleontrile acceptors.[8,13,16] The results obtained from p-DSCs also confirm that using thiophenes as π-linkers can enhance the electronic

communication within the dye, which is consistent with the series of triphenylamine-donor dyes reported by Ji *et al*. rather than the series of Qin *et al*.[13,14]

To the best of our knowledge this is the first reported use of rR to probe the excited state electronic structure of organic dyes adsorbed onto NiO. The rR spectra highlighted differences in the degree of electron density transferred to the electron acceptor in each dye. The low intensity of the vibrational modes corresponding to the maleonitrile groups in the spectra for **1**|NiO compared to the bodipy vibrations in the spectra for **2**|NiO and **3**|NiO illustrate that, strikingly, the charge accepting moieties that are successfully employed for triphenylamine dyes are not necessarily suitable for use with the pyrrole anchoring group. While the bodipy analogues, **2**|NiO and **3**|NiO, achieved effective charge separation at 476 nm, higher energy was required to excite **1**|NiO. Therefore competition for light with the NiO and iodide/triiodide electrolyte also contributed to the poor performance of p-DSCs incorporating **1**.

A comparison of the solar cell performance with the rR spectra suggests that there may be a correlation between the strength of the electronic coupling and the photocurrent generated. For systems such as **P1** the push-pull character extends beyond the dye when it is adsorbed onto NiO and charge-separation is very efficient. However, the bodipy dyes here are decoupled from the anchoring group and the excited states are more localised. When a thiophene bridge was used, the electron density extends onto the π-linker and an improvement in solar cell performance is observed. These results are in agreement with our recent study of triphenylamine-bodipy conjugates, in which we also observed an improvement in solar cell performance when the CH_3 substituents in positions 3 and 5 were replaced with H.[31] While generating a NiO-to-dye charge transfer state favours charge-separation it may also increase the hole-electron recombination, shortening the charge-separated state lifetime. We propose that a systematic correlation of rR and DSSC performance would be viable and highly useful.

Acknowledgements

Dr Raphael Horvath and Pritesh Tailor for their very helpful discussions. COST Action CM1202, the EPSRC, the Royal Society for a Dorothy Hodgkin Fellowship, the Leverhulme Trust (Project Grant RGS108374), the Studienstiftung des Deutschen Volkes for funding.

References

1 J. He, H. Lindström, A. Hagfeldt, S. Lindquist, *J. Phys. Chem. B.* **1999**, *103*, 8940–8943.

2 J. He, H. Lindström, A. Hagfeldt, S. Lindquist, *Sol. Energy Mater. Sol. Cells* **2000**, *62*, 265–273.

3 A. Morandeira, G. Boschloo, A. Hagfeldt, L. Hammarström, *J. Phys. Chem. B.* **2005**, *109*, 19403–10.

4 P. Qin, J. Wiberg, E. A. Gibson, M. Linder, L. Li, T. Brinck, A. Hagfeldt, B. Albinsson, L. Sun, *J. Phys. Chem. C.* **2010**, *114*, 4738–4748.

5 A. L. Smeigh, L. Le Pleux, J. Fortage, Y. Pellegrin, E. Blart, F. Odobel, L. Hammarström, *Chem. Commun.* **2012**, *48*, 678–80.

6 F. Odobel, Y. Pellegrin, E. A. Gibson, A. Hagfeldt, A. L. Smeigh, L. Hammarström, *Coord. Chem. Rev.* **2012**, *256*, 2414–2423.

7 P. Qin, H. Zhu, T. Edvinsson, G. Boschloo, A. Hagfeldt, L. Sun, *J. Am. Chem. Soc.* **2008**, *130*, 8570–1.

8 J.-F. Lefebvre, X.-Z. Sun, J. A. Calladine, M. W. George, E. A. Gibson, *Chem. Commun.* **2014**, *50*, 5258–60.

9 M. Bräutigam, M. Schulz, J. Inglis, J. Popp, J. G. Vos, B. Dietzek, *Phys. Chem. Chem. Phys.* **2012**, *14*, 15185–90.

10 A. Nattestad, A. J. Mozer, M. K. R. Fischer, Y.-B. Cheng, A. Mishra, P. Bäuerle, U. Bach, *Nat. Mater.* **2010**, *9*, 31–5.

11 S. Powar, T. Daeneke, M. T. Ma, D. Fu, N. W. Duffy, G. Götz, M. Weidelener, A. Mishra, P. Bäuerle, L. Spiccia, U. Bach, *Angew. Chem. Int. Ed.* **2013**, *52*, 602–5.

12 I. R. Perera, T. Daeneke, S. Makuta, Z. Yu, Y. Tachibana, A. Mishra, P. Bäuerle, C. A. Ohlin, U. Bach, L. Spiccia, *Angew. Chem.* **2015**, *127*, 3829–3833.

13 Z. Ji, G. Natu, Z. Huang, Y. Wu, *Energy Environ. Sci.* **2011**, *4*, 2818-2821.

14 P. Qin, M. Linder, T. Brinck, G. Boschloo, A. Hagfeldt, L. Sun, *Adv. Mater.* **2009**, *21*, 2993–2996.

15 S. Ngwerume, J. E. Camp, *J. Org. Chem.* **2010**, *75*, 6271–4.

16 L. Li, E. A. Gibson, P. Qin, G. Boschloo, M. Gorlov, A. Hagfeldt, L. Sun, *Adv. Mater.* **2010**, *22*, 1759–62.

17 M. Wächtler, J. Guthmuller, L. González, B. Dietzek, *Coord. Chem. Rev.* **2012**, *256*, 1479–1508.

18 M. K. Nazeeruddin, S. M. Zakeeruddin, R. Humphry-Baker, M. Jirousek, P. Liska, N. Vlachopoulos, V. Shklover, C. Fischer, M. Grätzel, *Inorg. Chem.* **1999**, *38*, 6298–6305.

19 L. C. T. Shoute, G. R. Loppnow, *J. Am. Chem. Soc.* **2003**, *125*, 15636–15646.

20 R Core Team, 2013.

21 T. Kupka, R. Wrzalik, G. Pasterna, K. Pasterny, *J. Mol. Struct.* **2002**, *616*, 17–32.

22 P. M. Viruela, R. Viruela, E. Ortí, J. Casado, V. Hernández, J. T. López Navarrete, *J. Mol. Struct.* **2003**, *651–653*, 657–664.

23 D. Collado, J. Casado, S. R. González, J. T. L. Navarrete, R. Suau, E. Perez-Inestrosa, T. M. Pappenfus, M. M. M. Raposo, *Chem. Eur. J.* **2011**, *17*, 498–507.

24 C. Kvarnström, A. Petr, P. Damlin, T. Lindfors, A. Ivaska, L. Dunsch, *J. Solid State Electrochem.* **2002**, *6*, 505–512.

25 J. D. Hall, T. M. McLean, S. J. Smalley, M. R. Waterland, S. G. Telfer, *Dalt. Trans.* **2010**, *39*, 437–445.

26 S. Badré, V. Monnier, R. Méallet-Renault, C. Dumas-Verdes, E. Y. Schmidt, A. I. Mikhaleva, G. Laurent, G. Levi, A. Ibanez, B. A. Trofimov, R. B. Pansu, *J. Photochem. Photobiol. A Chem.* **2006**, *183*, 238–246.

27 S. Ayachi, K. Alimi, M. Bouachrine, M. Hamidi, J. Y. Mevellec, J. P. Lère-Porte, *Synth. Met.* **2006**, *156*, 318–326.

28 S. Sumikura, S. Mori, S. Shimizu, H. Usami, E. Suzuki, *J. Photochem. Photobiol. A Chem.* **2008**, *199*, 1–7.

29 U. B. Cappel, S. M. Feldt, J. Schöneboom, A. Hagfeldt, G. Boschloo, *J. Am. Chem. Soc.* **2010**, *132*, 9096–101.

30 E. A. Gibson, L. Le Pleux, J. Fortage, Y. Pellegrin, E. Blart, F. Odobel, A. Hagfeldt, G. Boschloo, *Langmuir* **2012**, *28*, 6485–93.

31 G. H. Summers, J.-F. Lefebvre, F. A. Black, E. Stephen Davies, E. A. Gibson, T. Pullerits, C. J. Wood, K. Zidek, *Phys. Chem. Chem. Phys.* **2016**, *18*, 1059–1070.